Optical implementation of the Hopfield model for two-dimensional associative memory

Ju-Seog Jang, Su-Won Jung, Soo-Young Lee, and Sang-Yung Shin

Department of Electrical Engineering, Korea Advanced Institute of Science and Technology, P.O. Box 150, Cheongryang, Seoul, Korea

Received February 17, 1987; accepted December 22, 1987

Optical implementation of Hopfield's neural network model [Proc. Natl. Acad. Sci. USA **79**, 2554 (1982)] for two-dimensional associative memory is discussed. Two-state neuron elements are represented by a twisted nematic liquid-crystal optical switch array, and three-dimensional holographic interconnections are realized with these elements. Unipolar connections, created by adding a constant to bipolar interconnections and compensating them with an input-dependent thresholding operation, are realized. The 16- (4×4) neuron system model acts as a content-addressable associative memory with error-correction capability.

Optical information processing based on neural network models[1–3] has received special attention from the computer community because of the large degree of parallelism that must be incorporated in next-generation computers. Recently Hopfield introduced a simple associative-memory model[4] for the operation of neural networks, and Psaltis and Farhat[5] and Farhat *et al.*[6] reported realization of this model using an optical vector–matrix multiplier to process one-dimensional binary images. For the massive parallelism of optics to be utilized fully, two-dimensional (2-D) optical associative memory is required. In this Letter, optical implementation of the Hopfield (outer-product) model for associative memory of 2-D binary images is reported.

The Hopfield model can be summarized as follows. A set of M binary vectors $\mathbf{V}^s$, each N bits long, is stored in a storage matrix:

$$T_{ij} = \sum_{s=1}^{M} (2V_i^s - 1)(2V_j^s - 1) \qquad \text{for } i \neq j, \tag{1a}$$

$$T_{ii} = 0. \tag{1b}$$

The matrix $\mathbf{T}$ can be used for the retrieval of stored information from erroneous or partial input vectors. The vector–matrix product

$$\hat{V}_i^t \equiv \sum_j T_{ij} V_j^t, \tag{2}$$

with the thresholding operation

$$V_i^t = 1 \qquad \text{if } \hat{V}_i^t \geq 0 \tag{3a}$$

$$= 0 \qquad \text{otherwise,} \tag{3b}$$

yields an estimate of the stored vector that is most like the input vector $\mathbf{V}_t$.[7] As is shown in Fig. 1, the thresholded estimate vector is fed back to the input and converges to the correct stored vector.

Since 2-D images are treated as matrices, Eq. (1) yields a fourth-rank tensor. However, it is difficult to implement such a fourth-rank tensor system directly. In Ref. 5 an extension of the Hopfield model for image storage was proposed that involved wavelength multiplexing, time-domain processing, or both. However, these solutions may actually add complexity to the system. On the other hand, the Hopfield model can be made applicable to 2-D images without any extension. The vector–matrix product, $\sum T_{ij}V_j$, corresponds physically to the interconnections of neurons, as shown by the dashed box in Fig. 1. We can rearrange the neurons in two dimensions and their interconnections in three dimensions (see Fig. 2). These matrix–matrix global interconnections can be implemented directly by using the focused or unfocused holographic interconnection method.[8] There are several types of 2-D holographic associative memory that use correlation and convolution between the input image and the output image.[9,10] Our system, shown in Fig. 3, uses the direct outer-product scheme and is realized with a 2-D optical switch array (or spatial light modulator), a 2-D detector array (or charge-coupled device detector), and unfocused holographic interconnections employing cell-by-cell thresholding operations. The $N \times N$ multielement hologram performs a projection operation. Each pixel in an $N \times N$ input pattern can either illuminate (if the pixel is on) or not illuminate (if it is off) a separate hologram

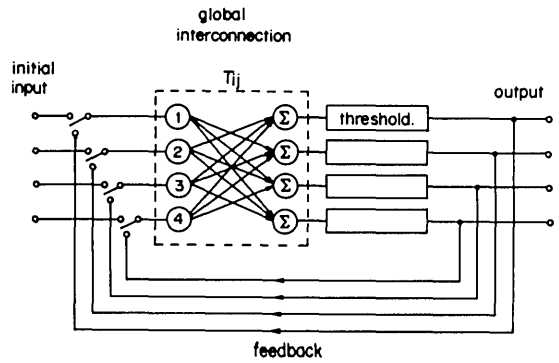

Fig. 1. Hopfield's neural network model.

0146-9592/88/030248-03$02.00/0

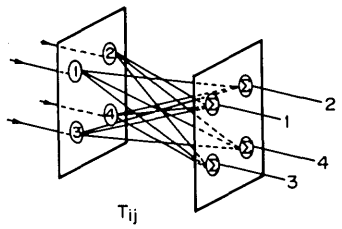

Fig. 2. Three-dimensional interconnections of neuron elements, T_{ij}: rearrangement of the neurons and their interconnections in the dashed box in Fig. 1.

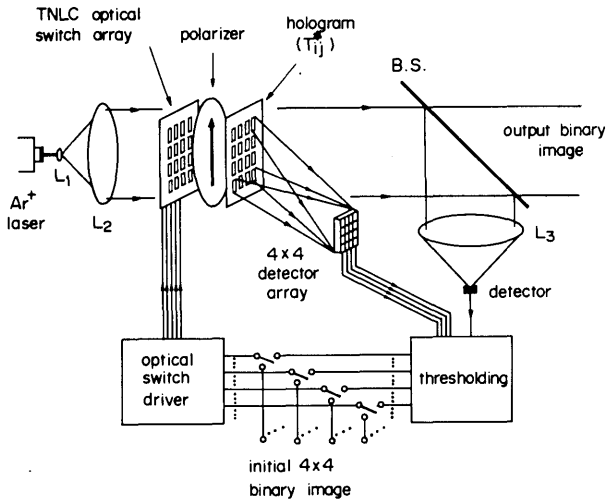

Fig. 3. Total setup of the system in which unfocused holographic interconnections are realized. B.S., beam splitter; L_1–L_3, lenses.

element positioned in front of it. Each hologram element contains an $N \times N$ connection pattern; the full set of connection patterns is $N^2 \times N^2$. The light from each element of the $N \times N$ connection hologram is projected onto a single $N \times N$ detector array to carry out summation. Cell-by-cell thresholding operations enhance the power and the contrast of the output image. Furthermore, the zeroth-order diffracted beam is itself the binary image output, and all first-order diffracted beams contribute to the interconnections of neuron elements. This system differs from other holographic associative memories[9,10] in which the zeroth-order diffracted beam is discarded and only the first-order diffracted beam is utilized in both the interconnections and the output.

It is inconvenient to build an optical system that contains both positive and negative T_{ij} connections. For example, Psaltis and Farhat use double photodetectors in each neuron and a double-row mask for connection matrix **T**. Following Denker,[11] we add a constant to T_{ij} to obtain unipolar T_{ij}^* and compensate it with an input-dependent thresholding operation as

$$\hat{V}_i^t \equiv \sum_j T_{ij}^* V_j^t, \tag{4}$$

$$V_i^t = 1 \quad \text{if } \hat{V}_i^t \geq \sum V_j^t \tag{5a}$$

$$= 0 \quad \text{otherwise,} \tag{5b}$$

where $T_{ij}^* = T_{ij} + 1$ for all i, j, and T_{ij} is assumed to be clipped. Figure 3 illustrates how the hologram (for T_{ij}^*) and the detector array execute the $\sum T_{ij}^* V_j^t$ operation and the beam splitter, lens L_3, and one detector execute $\sum V_j^t$. Thresholded outputs are fed back to drive twisted nematic liquid-crystal (TNLC) switches, which either pass or block the laser beams. Since T_{ij}^* is unipolar (0, 1, 2), only $N + 1$ photodetectors and N connection patterns are needed for an N-neuron system. Note that $2N$ photodetectors and $2N$ connection patterns are required for N-neuron systems with both excitatory and inhibitory interconnections.

In an experiment two binary images,

$$X \equiv \begin{bmatrix} 1 & 0 & 0 & 1 \\ 0 & 1 & 1 & 0 \\ 0 & 1 & 1 & 0 \\ 1 & 0 & 0 & 1 \end{bmatrix}, \qquad C \equiv \begin{bmatrix} 0 & 1 & 1 & 1 \\ 0 & 1 & 0 & 0 \\ 0 & 1 & 0 & 0 \\ 0 & 1 & 1 & 1 \end{bmatrix}, \tag{6}$$

are stored in the 16- (4×4) neuron system. As shown in Fig. 2, we consider two one-dimensional binary vectors,

$$\mathbf{V}^1 = [1\,0\,0\,1 \quad 0\,1\,1\,0 \quad 0\,1\,1\,0 \quad 1\,0\,0\,1]^T, \tag{7a}$$

$$\mathbf{V}^2 = [0\,1\,1\,1 \quad 0\,1\,0\,0 \quad 0\,1\,0\,0 \quad 0\,1\,1\,1]^T, \tag{7b}$$

which are rearranged to become the stored X and C images such that $\mathcal{T}[\mathbf{V}^1] = X$ and $\mathcal{T}[\mathbf{V}^2] = C$. The 16×16 T_{ij}^* matrix is calculated from vectors $\mathbf{V}^1$ and $\mathbf{V}^2$. Each row (or column) of T_{ij}^* ($= T_{ji}^*$) is also transformed with the same transformation, $\mathcal{T}$. These 16 transformed connection patterns are shown in Fig. 4. Black, gray (mosaic), and white (transparency) correspond to 0, 1, and 2, respectively. Each 4×4 connection pattern is sequentially recorded in separate 4×4 hologram elements through a contacted mask having a

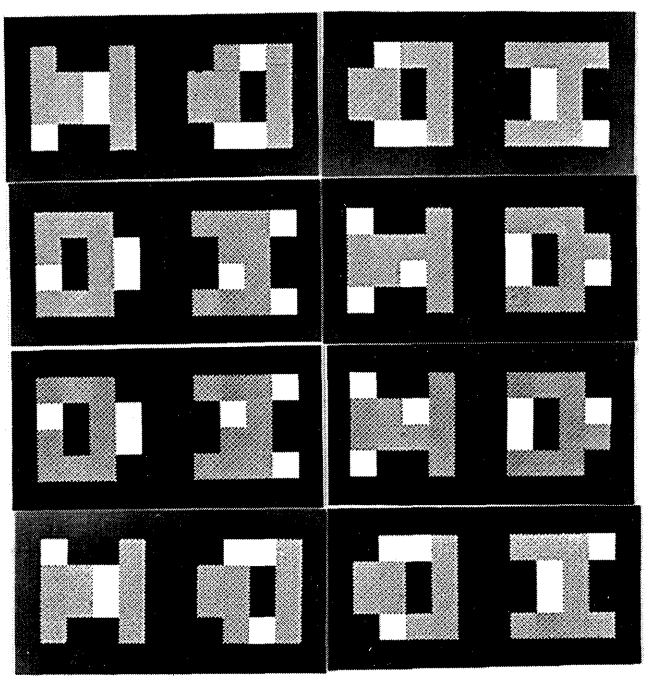

Fig. 4. Sixteen 2-D connection patterns fabricated on black background.

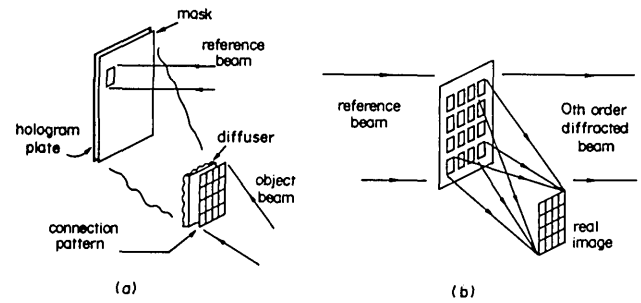

Fig. 5. Hologram recording and reading for T_{ij}*: (a) recording, (b) reading.

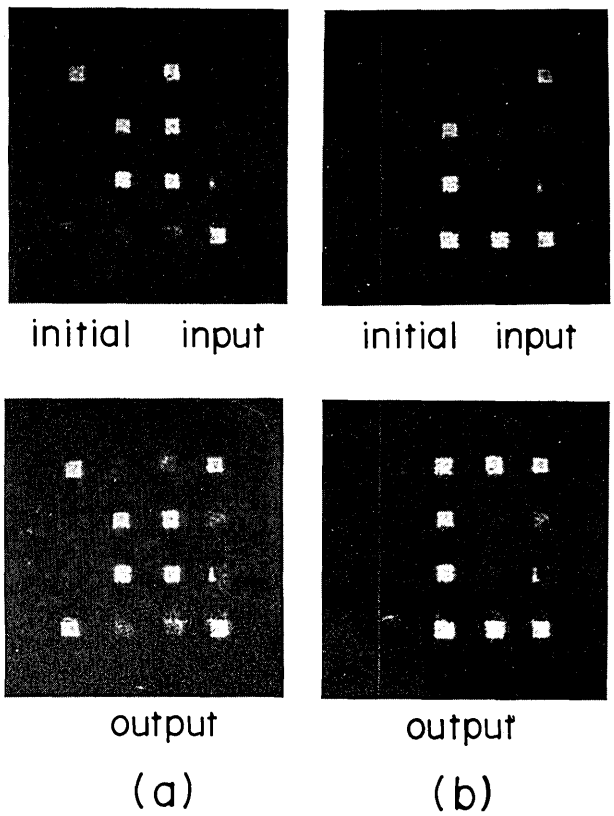

Fig. 6. Experimental results: (a) X image, (b) C image.

square opening (3 mm × 3 mm) that blocks noise illumination on other hologram elements. The method of recording and reading is shown in Fig. 5. The diffuser is used to randomize the phases so that noncoherent addition can be performed in the detector array. This phase averaging is effective if the size of the connection pattern is sufficiently larger than the size of the diffuser grain.

Although the number of neurons in this system is small, there is considerable error-correction capability. A few results are shown in Fig. 6 for images X and C. (Inverse images, $\bar{X}$ and $\bar{C}$, are similarly retrievable.) When an initial image contains fewer than 3 bit errors, this system finds the stored image that has the shortest Hamming distance from the input image. Errors larger than 4 bits either yield random convergence to one of the stored images or give outputs with one or more oscillating bits. All high initial images generate erratic patterns, which do not converge.

The switching time of the TNLC optical switches (or liquid-crystal displays) is about 100 msec. High-speed optical switches, such as integrated thin-film optical bistable devices,[12] may improve the speed. Programmable 2-D associative memory can be realized with the help of a dynamic volume hologram. Realization of a practical number of neurons, e.g., 1000 (30 × 30), is possible in our scheme. The important factors for large-scale implementation are the resolution of the hologram plate, the size of the connection pattern, the distance between the plate and the connection pattern, and the size of the hologram elements (see Fig. 5). We found that about 30 × 30 neurons can easily be interconnected with a reasonably sized (3 cm × 3 cm with a cell size of 1 mm × 1 mm) hologram plate. Computer-generated holograms may be used for similar interconnections.

In conclusion, we have optically implemented the Hopfield model (outer-product model) for 2-D binary-image associative memory by using a three-dimensional holographic interconnection method. We used a unipolar connection matrix $\mathbf{T}^*$ with an input-dependent thresholding operation. We discussed the advantages of this system and demonstrated its error-correction capability.

The authors acknowledge the reviewers' helpful comments, which improved this Letter.

References

1. M. Takeda and J. W. Goodman, Appl. Opt. **25,** 3033 (1986).
2. J. J. Hopfield and D. W. Tank, Science **233,** 625 (1986).
3. R. A. Athale, H. H. Szu, and C. B. Friedlander, Opt. Lett. **11,** 482 (1986).
4. J. J. Hopfield, Proc. Natl. Acad. Sci. USA **79,** 2554 (1982).
5. D. Psaltis and N. Farhat, Opt. Lett. **10,** 98 (1985).
6. N. Farhat, D. Psaltis, A. Prata, and E. Paek, Appl. Opt. **24,** 1469 (1985).
7. B. Macukow and H. H. Arsenault, Appl. Opt. **26,** 924 (1987).
8. J. W. Goodman, F. J. Leonberger, S.-Y. Kung, and R. A. Athale, Proc IEEE **72,** 850 (1984).
9. E. G. Paek and D. Psaltis, Opt. Eng. **26,** 428 (1987).
10. Y. Owechko, G. J. Dunning, E. Marom, and B. H. Soffer, Appl. Opt. **26,** 1900 (1987).
11. J. S. Denker, AIP Conf. Proc. **151,** 121 (1986).
12. T. Venkatesan, B. Wilkens, Y. H. Lee, M. Warren, G. Olbright, H. M. Gibbs, N. Peyghambarian, J. S. Smith, and A. Yariv, Appl. Phys. Lett. **48,** 145 (1986).